

Theoretical studies of spin-dependent electronic transport in ferromagnetically contacted graphene flakes

S. Krompiewski¹

¹Institute of Molecular Physics, Polish Academy of Sciences,
ul. M. Smoluchowskiego 17, 60179 Poznań, Poland

(Dated: April 2, 2024)

Based on a tight-binding model and a recursive Green's function technique, spin-dependent ballistic transport through tiny graphene sheets (flakes) is studied. The main interest is focused on: electrical conductivity, giant magnetoresistance (GMR) and shot noise. It is shown that when graphene flakes are sandwiched between two ferromagnetic electrodes, the resulting GMR coefficient may be quite significant. This statement holds true both for zigzag and armchair chiralities, as well as for different aspect (width/length) ratios. Remarkably, in absolute values the GMR of the armchair-edge graphene flakes is systematically greater than that corresponding to the zigzag-edge graphene flakes. This finding is attributed to the different degree of conduction channel mixing for the two chiralities in question. It is also shown that for big aspect ratio flakes, 3-dimensional end-contacted leads, very much like invasive contacts, result in non-universal behavior of both conductivity and Fano factor.

PACS numbers: 81.05.Uw, 75.47.De, 75.47.Jn

I. INTRODUCTION

Recently a lot of interest has been directed to carbon-based systems, in search for alternative materials which would make it possible to go beyond the silicon technology. While looking at history of studies along this line, one can point out two important milestones: (i) discovery of carbon nanotubes (CNTs), honeycomb-lattice cylinders, dating back to 1991,¹ and (ii) fabrication of individual atomic planes, called graphene (Gr), by exfoliation from graphite in 2004.² So far, on obvious grounds, the CNTs have been much more thoroughly investigated than Gr, but this difference diminishes very quickly. This paper focusses on spin transport problems, mostly on giant magnetoresistance, related to potential applications of graphitic nanostructures in spintronics. In this respect, quite a lot has been done in the case of CNTs, there are hundreds of both experimental^{3,4,5,6,7} and theoretical^{8,9,10,11} papers, covering all the transport regimes (ballistic, Coulomb blockade, Schottky barrier and Kondo) which show that the GMR or TMR (T for tunnel) effects are usually quite considerable. The respective studies on Gr are still scarce. The pioneering experimental paper on magnetoresistance is Ref.[12], where Gr spin valve devices with permalloy contacts have been shown to have the GMR effect ~ 10% at room temperature. The following experimental paper,¹³ reports on conductance of Gr showing Fabry-Pérot-like patterns, and pronounced oscillations of GMR (including changes in sign). From the theoretical point of view, the debate is still on, and the question whether or not the Gr-based spin valves have a good performance is still open. The results published so far show that the answer to this question depends critically on the contacts (cf. Ref.[14] and Refs.[15,16]). In this study, in contrast to those reported

hitherto by other theoreticians, a 3-dimensional contacts are used.

The paper is organized as follows: In Sec. II the theoretical method based on a tight-binding model, as well as the way the graphene sheets and the contacts have been modelled, are shortly outlined. Sec. III is devoted to presentation of results, whereas the subsequent section summarizes the main results.

II. METHOD AND MODELLING

The method employed here is similar to that used earlier while dealing with carbon nanotubes inserted between ferromagnetic contacts,^{9,10,11} except that carbon allotrope of interest now is graphene. The single-orbital tight-binding Hamiltonian describes a graphene sheet of width W and length L (in the current direction). The semi-infinite metallic electrodes extend from $x < 0$ and $x > L$ for the source and drain, respectively. The ferromagnetic electrodes are supposed to have spin-split s -bands, mimicking d -bands of real transition metals. The total Hamiltonian reads

$$H = \sum_{i,j} t_{i,j} \tilde{c}_i^\dagger c_j + \sum_i \epsilon_i c_i^\dagger c_i \quad (1)$$

where i and j run over the whole device (i.e. graphene and the electrodes), ϵ_i is the spin index, and $t_{i,j}$ and ϵ_i stand for the hopping integrals and the on-site potentials, respectively. The systems under study are in purity-free with well transparent interfaces (strong coupling limit) so neglecting of correlations in the Hamiltonian should be

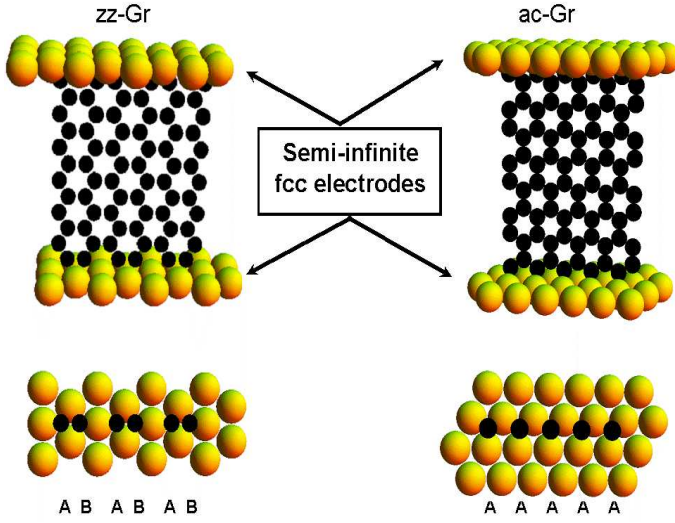


FIG. 1: (Color online) Graphene sheets attached to semi-infinite 3-dimensional metallic electrodes. The left and right parts correspond to the zigzag- and arm chair-edge ribbons, respectively. The lower part shows details of the interfaces, whereas the letters A, B denote a type of the sublattice the interface carbon atoms belong to.

justified if one restricts oneself just to the ballistic transport regime, putting aside the Coulomb blockade^{6,17} and Kondo^{5,7} regimes. In this regard, the on-site parameters in the present approach are used to take into account the effect of the gate voltage in the graphene sheet as well as the spin band-splitting in the metallic electrodes.

Fig. 1 shows schematically devices of the present interest, viz. zigzag-edge graphene (zz-Gr) and arm chair-edge graphene (ac-Gr). The graphene sheets (black spheres) are sandwiched between metallic contacts (light spheres). The diameters of the spheres correspond to the nearest neighbor spacings. The unit cells in the vertical direction are the blunt saw-teeth lines for zz-Gr, and double zigzag lines for ac-Gr. As readily seen, it is assumed that there is a perfect lattice matching between graphene and the electrodes. In fact this assumption is acceptable since the graphene lattice constant ($a_{Gr} = 2.46 \text{ \AA}$) fits really well to interatomic distances in such metals like: Cu (2.51 \AA), Ni (2.49 \AA) or Co (2.55 \AA).¹⁸

The use of a single-orbital electrodes allows to write an analytic expression for the electrodes surface Green

functions in k -space.

$$g(k; E) = \frac{E - \epsilon(k)}{2jv(k)^2} \frac{P}{(E - \epsilon(k))^2 - 4jv(k)^2} \quad (1)$$

$$\epsilon(k) = 2t(\cos k_x a + 2 \cos \frac{k_x a}{2} \cos \frac{3k_y a}{2}) +$$

$$w(k) = t(2 \cos \frac{k_x a}{2} e^{\frac{ik_y a}{3}} + e^{\frac{ik_y a}{3}}); \quad (2)$$

where $a = 2a_{Gr}$ is the fcc-metal lattice constant, g is the surface Green function for spin σ , and $\epsilon(k)$ is a rigid band splitting chosen so as to give a desirable spin polarization P of the electrodes. Here $P = 50\%$ has been set, corresponding to $t = 2.32t$ and $\epsilon = 1.6t$ (in the paramagnetic case $\epsilon = 0.86t$). Incidentally, this simple parametrization has already been shown to work satisfactorily well in the case of carbon nanotube/ferromagnet systems.^{9,10} $\epsilon(k)$ in Eq. (2) is the fcc(111)-surface energy spectrum, calculated for a semi-infinite metal slab according to the method described in Ref. [19]. The surface k -vectors lie on the metal surface but upon attachment of graphene they are no longer good quantum numbers, so the trick is to perform a Fourier transformation to the real space and work with those surface Green function which are close to the graphene interface. After having transformed the surface Green function to the real-space, the self-energies and the corresponding spectral functions are computed from $\Sigma = TgT^\dagger$ and $\rho = i(\Sigma^{-1} - \epsilon^{-1})$, respectively. With $i = L$ or R , referring the left and right electrodes, and T being the Gr/electrode coupling matrices. Henceforth, the spin indexes will be skipped for brevity.

The recursive method goes as follows²⁰

$$g_L(0) = g_L; \quad g_R(N+1) = g_R;$$

$$g_{L,R}(i) = (E - D_{i,i} - T_{i,i} g_{L,R}(i+1))^{-1}$$

$$T_L(i) = T_{i,i+1} g_L(i+1) T_{i+1,i};$$

$$T_R(i) = T_{i,i+1} g_R(i+1) T_{i+1,i}; \quad (3)$$

$$G_i = (E - D_{i,i} - T_{i,i} g_L(i) - T_{i,i} g_R(i))^{-1}; \quad (4)$$

Above, $g_{L,R}$ are local Green's functions for the i -th unit cell of graphene, the matrices D and T stand for the diagonal and off-diagonal Hamiltonian submatrices, whereas the full Green's function is given by Eq. 4. The graphene unit cells extend from $i = 1$ (following the L electrode) up to $i = N$ (preceding the R electrode). So the recursion starts with the metal-interface Green functions $g_L(0)$ and $g_R(N+1)$ being Fourier components of the surface Green functions defined in Eq. (2).

The other quantities of interest are transmission (T), conductivity (σ), and shot noise Fano factor (F), as well as giant magnetoresistance (GMR). In the ballistic transport regime and at zero temperature these quantities read:

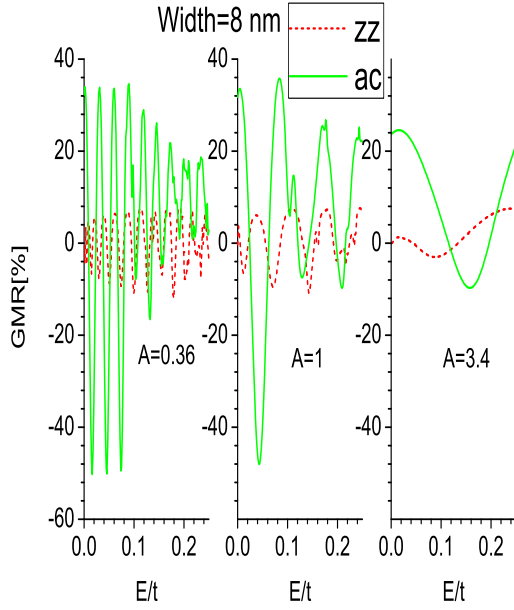


FIG. 2: (Color online) Giant magnetoresistance for ac-Gr (solid curve) and zz-Gr (dash curve) as vs energy, and for 3 different aspect ratios. Note that the number of quasi-periods is roughly inverse proportional to A (i.e. proportional to the length), meaning that Fabry-Pérot-like resonances take place.

$$\begin{aligned}
 T &= \frac{L}{i} G_i^R \frac{R}{i} G_i^L; \\
 &= (L=W) \frac{e^2}{h} \text{Tr}[T(E_F)]; \\
 F &= \text{Tr}[T(E)(1 - T(E))] / \text{Tr}[T(E)]; \\
 \text{GMR} &= 100(1 - \frac{F}{F_0}); \quad (5)
 \end{aligned}$$

where the arrows " \parallel " and " $\#$ " denote parallel and antiparallel alignments of ferromagnetic electrodes.

III. RESULTS

We use Eqs 5 to determine the quantities of our main interest. At first, for comparison, we have calculated GMR for zz- and ac-Gr sheets vs. energy which, in principle, is proportional to the gate voltage. From the results in Fig 2 one can see that GMR, at least in the ac-Gr case, is quasi-periodic with the period-length roughly proportional to the aspect ratio A , i.e. inverse proportional to the length of the graphene sheets L . Numerically, the periods are close to the well-established value $p = 2\text{eV} / L [\text{nm}]$,²¹ or in the present units $p = 0.8 A / W [\text{nm}]$ (the energy unit is $t = 2.7 \text{ eV}$). Incidentally, some features characteristic for Fabry-Pérot resonances in graphene have been already reported^{21,22}, where it has been also stressed that irregularities and defects of graphene-edges may turn the con-

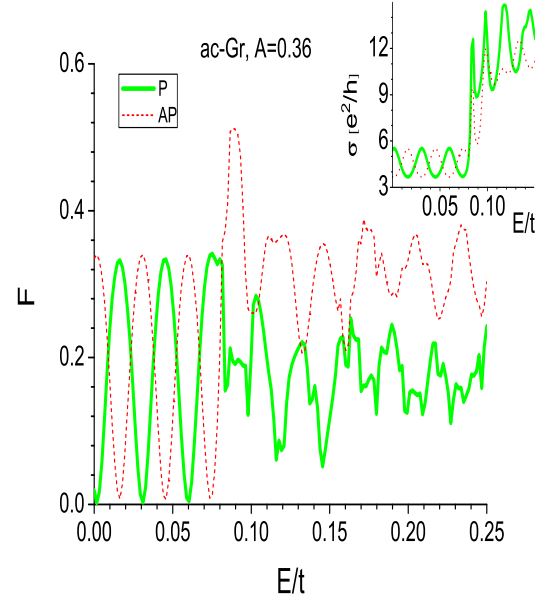


FIG. 3: (Color online) Shot noise Fano factor for the arm chair graphene ca 8nm in width and with the aspect ratio $A = 0.36$: for ferromagnetic electrodes (parallel alignment – thin solid line, and antiparallel alignment – dash line). Inset presents the respective conductivities.

ventional Fabry-Pérot picture into a spectacular quantum billiard-type one. It is seen in Fig. 2 that the GMR factors for ac-Gr and zz-Gr differ in 3 respects: (i) magnitude, (ii) the maxima of the former are roughly equidistant in contrast to the latter, moreover (iii) in the former the onset of the second sub-band is visible (at $E = 0.08$, except for $A = 3.4$, where $W > L$), whereas in the latter it always is washed out. Qualitatively these results, showing that GMR vs. energy (gate voltage) changes also in sign, are consistent with the experiment of Ref. [13].

Another interesting point encountered here, is the universal behavior issue due to evanescent modes at the Dirac points. It is well-known that graphene sheets of large sizes, with $W \gg 1$ and $L \gg 1$ (with $W > L$), if homogenous, reveal universal values of $F = 4 = e^2/h$ and $F = 1 = 3$.^{21,25,26} The term "homogenous" in this context means that the device at hand is an all-carbon system, typically, with a central graphene sheet, and highly doped graphene electrodes. This theoretical concept might be quite realistic for widely applied experimental setups with side-contacted graphene sheets, provided evaporated metal contacts are not invasive, i.e. they do not destroy the underlying honey-comb lattice but merely dope it slightly. It has been also shown theoretically that in the case of end-contacted devices to 2-dimensional square-lattice contacts, the situation is more complicated and respective values of the conductivity and the Fano factor do depend on the on-site potentials in electrodes and on details of bonds between square-lattice electrodes and graphene.²⁷ Importance of

the interface conditions which determine, inter alia, mixing of propagating modes, and whether or not the momentum component along the interface direction is conserved, has been noticed in Ref.[27,28,29,30,31,32]. It has been also demonstrated using one-parameter scaling arguments that at the Dirac points, conductivity of an infinitely large graphene with disorder is infinite (zero) if there is not (there is) intervalley scattering.²³ Beyond the Dirac points the evanescent modes give way to the propagating ones, and in the ballistic transport regime, perfect noiseless transmission due to Fabry-Pérot resonances may take place.^{13,24}

Fig.3 clearly shows that this scenario also holds in the ferromagnetic case for ac-Gr if the aspect ratio is not too big (Gr ribbon is long enough). Indeed maxima in

(Inset) correspond to minima of F (at $F=0$) in the main panel. In the zz-Gr case with the same A value the situation is similar (not plotted), but then the oscillations in the P and AP configurations are not phase-shifted.

As regards Gr sheets with bigger A , Figs.4 and 5 show some features of F and σ which happen to be similar to the universal ones when the Gr sheets are paramagnetically contacted (thick black lines). However, if the contacts are ferromagnetic there is a tendency for F to increase and for σ to decrease. This suggests that in general Gr-akes studied here show non-universal behavior, which is to be attributed to the finite sizes, and the inhomogeneity resulting in contact-dependent charge transfer between interface atoms (and accompanying electron-hole asymmetry). Incidentally, the present approach was shown earlier to yield short-range charge transfer, affecting mainly interface carbon monolayers.^{10,20} As a matter of fact, the non-universal behavior of F and σ in Gr-systems has been already reported to be due to: charged impurity scattering,³⁴ strong disorder³⁵, invasive contacts.^{36,37}

Finally, it should be noted that the results presented in Figs. 2-5 hardly depend on the hopping parameters as long as the interfaces are transparent enough. In the present theory this condition is fulfilled provided the hopping parameter across the interface (t_c) is not too different from the geometric mean of hopping parameters for the metal electrodes (t_M) and graphene (t), i.e. from $t_c = \sqrt{t_M t}$. Otherwise, in case of a drastic differentiation of the hopping parameters, and opaque interfaces (very small t_c) the Coulomb blockade physics may come into play,¹⁷ out of reach of the present approach.

IV. CONCLUSION

Summarizing, the aim of this study has been to estimate the effect of the chirality as well as the aspect ratio on the GMR coefficient of graphene flakes end-contacted to ferromagnetic electrodes. In contrast to other theoretical approaches, the leads are not supposed here to be

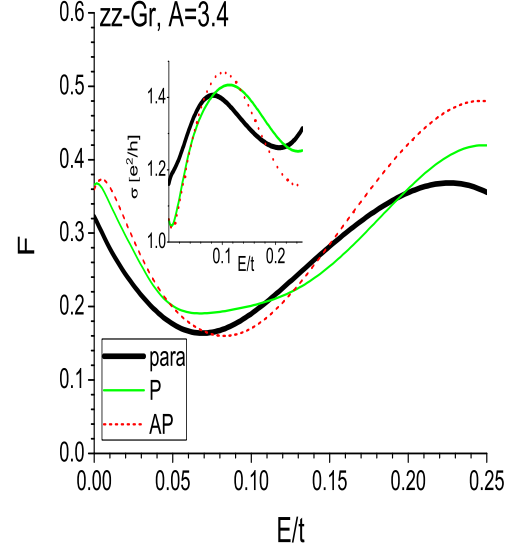


FIG. 4: (Color online) Shot noise Fano factor for the zigzag-edge graphene ca 8nm in width and with the aspect ratio $A=3.4$: for paramagnetic electrodes (thick solid line), ferromagnetic electrodes (parallel alignment – thin solid line, and antiparallel alignment – dash line). Inset presents the respective conductivities.

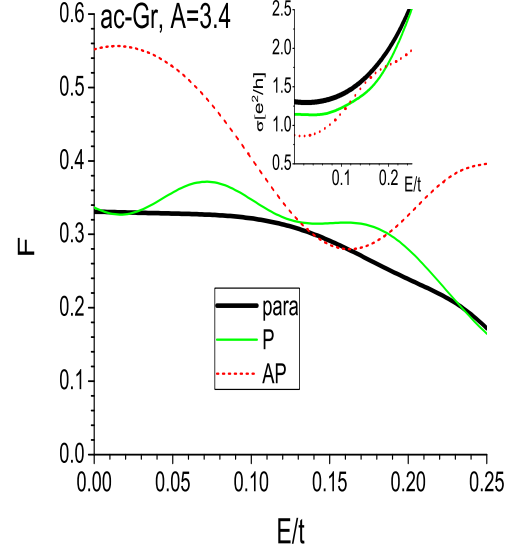


FIG. 5: (Color online) As 4 but for armchair-edge graphene.

two-dimensional (of honeycomb- or square-lattice type), but more realistically they are modelled as 3-dimensional fcc-(111) semi-infinite slabs. It turns out that for long and narrow systems (small aspect ratio), the GMR is a quasi-periodic function of energy (gate voltage) with the period roughly proportional to the aspect ratio, re-

ecting Fabry-Perot-like resonances, typical of ballistic transport. Notably, the GM R coefficient of the ac-G rakes may exceed 20% – 40%, depending on the aspect ratio value, whereas for zz-G rakes the corresponding figures are distinctly smaller, but still significant. The difference is due to the fact that in the case of arm chair-edge sheets all the interface carbon atoms belong to the same sub-lattice (say, A-type), as opposed to the zigzag ones with interface carbon atoms of both A- and B-type. This inevitably facilitates intervalley mode mixing in the latter case. Another noteworthy point, in the context of zero-energy (Dirac-point) conductivity and Fano factor, is that for the big aspect ratio. Such systems studied here show non-universal behavior when ferromagnetic electrodes are applied. It is so even if the corresponding values for the paramagnetic electrodes happen to be close to the universal ones ($4 = e^2/h$ and $1/3$ for \uparrow and \downarrow , respectively). However, these systems are inhomogeneous and rather small, so neither the limits $W \rightarrow 1$ and $L \rightarrow 1$ (with $W > L$), nor the requirement of a large

number of propagating modes can be fulfilled (see the relevant assumptions in Ref[25]). It is noteworthy that the wide end-contacted devices considered here resemble experimental setups with invasive contacts, which do not show universal behavior, either.

V. ACKNOWLEDGMENTS

This work was supported by the EU FP6 grant CARDEQ under contract No. IST-021285-2; and, as part of the European Science Foundation EUROCORES Programme SPINTRA (contract No. ERAS-CT-2003-980409), by the Ministry of Science and Higher Education as a research project in 2006-2009.

References

- ¹ S. Iijima, *Nature* (London), 354, 56 (1991).
- ² K.S. Novoselov, A.K. Geim, S.V. Morozov, D. Jiang, Y. Zhang, S.V. Dubonos, I.V. Grigorieva, A.A. Firsov, *Science* 306, 666 (2004) (2004).
- ³ K. Tsukagoshi, B.W. A. Jphenaar, and H. Ago, *Nature* 401, 572 (1999).
- ⁴ S. Sahoo, T. Kontos, J. Furer, C. Hermann, M. Graber, A. Cottet, and C. Schonenberger, *Nature Physics* 1, 99 (2005).
- ⁵ J.R. Hauptmann, J. Paaske, and P.E. Lindelof, *Nature Physics* 4, 373 (2008).
- ⁶ W. Liang, M. Bockrath, and H. Park, *Phys. Rev. Lett.* 88, 126801 (2002).
- ⁷ S. Samin, P. Jarillo-Herrero, J. Kong, C. Dekker, L.P. Kouwenhoven, and H.S.J. van der Zant, *Phys. Rev. B* 71, 153402 (2005).
- ⁸ H. Mehrez, J. Taylor, H. Guo, J. Wang, and C. Roland, *Phys. Rev. Lett.* 84, 2682 (2000).
- ⁹ S. Krompiewski, *physica status solidi (b)*, 242 226 (2005).
- ¹⁰ S. Krompiewski, *Semicond. Sci. Technol.* 21 S96 (2006).
- ¹¹ S. Krompiewski, *Nanotechnology* 18, 485708 (2007).
- ¹² E. Hill, A.K. Geim, K. Novoselov, F. Schedin, and P. Blake, *IEEE Trans. Magn.* 42, 2694 (2006).
- ¹³ S. Cho, Yung-Fu Chen, and M. S. Fuhrer, *Appl. Phys. Lett.* 91, 123105 (2007).
- ¹⁴ L. Brey and H.A. Fertig, *Phys. Rev. B*, 76, 205435 (2007).
- ¹⁵ Woo Youn Kim and Kwang, S. Kim, *Nature Nanotech.*, 408 3 (2008).
- ¹⁶ K.H. Ding, Z.G. Zhu, and J. Berakdar, *Phys. Rev. B*, 79, 045405 (2009).
- ¹⁷ I. Weymann, J. Bamas, and S. Krompiewski, *Phys. Rev. B*, 78, 035422 (2008).
- ¹⁸ V.M. Karpan, G. Giovannetti, P.A. Khomyakov, M. Talaranana, A.A. Starikov, M. Zwierzycki, J. van den Brink, G. Brocks, and P.J. Kelly, *Phys. Rev. Lett.* 99, 176602 (2007).
- ¹⁹ T.N. Todorov, G.A.D. Briggs, and A.P. Sutton, *J. Phys. Condens. Matter* 5, 2389 (1993).
- ²⁰ S. Krompiewski, *J. Phys.: Condens. Matter* 16, 2981 (2004).
- ²¹ F. Miao, S. W. Jijratne, Y. Zhang, U.C. Coskun, W. Bao, C.N. Lau, *Science*, 317, 1530 (2007).
- ²² L.A. Ponomarenko, F. Schedin, M.I. Katsnelson, R. Yang, E.W. Hill, K.S. Novoselov, and A.K. Geim, *Science* 320, 356 (2008).
- ²³ J.H. Bardarson, J. Tworzydło, P.W. Brouwer, and C.W. J. Beenakker, *Phys. Rev. Lett.* 99, 106801 (2007).
- ²⁴ J. Cayssol, B. Huard, and D. Goldhaber-Gordon, *cond-mat/0810.4568*.
- ²⁵ J. Tworzydło, B. Trauzettel, M. Titov, A. Rycerz, and C.W. J. Beenakker, *Phys. Rev. Lett.* 96, 246802 (2006).
- ²⁶ R. D'anneau, F. Wu, M.F. Craciun, S. Russo, M.Y. Tom, J. Salmilehto, A.F. Morpurgo, and P.J. Hakonen, *Phys. Rev. Lett.* 100, 196802 (2008).
- ²⁷ R.L. Dragomirova, D.A. Arshkin, and B.K. Nikolic, *Phys. Rev. B* 79, 241401(R) (2009).
- ²⁸ Ya.M. Blanter and I. Martin, *Phys. Rev. B* 76, 155433 (2007).
- ²⁹ J.P. Robinson and H. Schonenberger, *Phys. Rev. B* 76, 115430 (2007).
- ³⁰ Eduardo J. H. Lee, Kannan Balasubramanian, Ralf Thomas Weitz, Marko Burghard, and Klaus Kem, *Nature Nanotech.*, 486 3 (2008).
- ³¹ Roksana Golizadeh-Mojarad and Supriyo Datta, *Phys. Rev. B* 79, 085410 (2009).
- ³² S. Russo, M.F. Craciun, M. Yamamoto, A.F. Morpurgo, and S. Tarucha, *cond-mat/0901.0485v1*.
- ³³ P. Blake, R. Yang, S.V. Morozov, F. Schedin, L.A. Ponomarenko, A.A. Zhukov, R.R. Nair, I.V. Grigorieva, K.S. Novoselov, A.K. Geim, *Solid State Comm.*, 149, 1068 (2009).
- ³⁴ J.-H. Chen, C. Jang, S. Adam, M. S. Fuhrer, E. D. Williams, and M. Ishigami, *Nature Physics* 4, 377 (2008).
- ³⁵ C.H. Lewenkopf, E.R. Mucciolo, and A.H. Castro Neto,

Phys. Rev. B, 77, 081410(R) (2008).

³⁶ B. Huard, N. Stander, J. A. Sulpizio, and D. Goldhaber-Gordon, Phys. Rev. B, 78, 121402(R) (2008).

³⁷ Xu Du, I. Skachko and E. Y. Andrei, cond-mat/0901.1420.